

E6-2015-41

I. N. Izosimov*

**ISOSPIN QUANTUM NUMBER AND STRUCTURE OF THE
EXCITED STATES IN HALO NUCLEI. HALO-ISOMERS**

Submitted to the International Conference
“Isospin, structure, reactions, and energy of symmetry, ”
ISTROS-2015, May 1–6, 2015, Casta-Papiernicka, Slovakia

* E-mail: izosimov@jinr.ru

Изосимов И. Н.

E6-2015-41

Изоспин и структура возбужденных состояний в галоидальных ядрах.
Гало-изомеры

Показано, что волновые функции изобар-аналоговых (IAS), дубль-аналоговых (DIAS), конфигурационных (CS) и дубль-конфигурационных (DCS) состояний могут одновременно содержать компоненты, соответствующие $n-n$, $n-p$ и $p-p$ гало. Различия в структуре гало для возбужденных состояний ядра и основного состояния могут приводить к образованию изомеров (гало-изомеров). Гало-структура как борромиеановского, так и танго типа может наблюдаться для $n-p$ конфигураций. Обсуждается структура основных и возбужденных состояний с различным изоспином в галоидальных ядрах. Проведен анализ приведенных вероятностей $B(M\lambda)$ и $B(E\lambda)$ гамма-переходов в ядрах ${}^{6-8}\text{Li}$, ${}^{8-10}\text{Be}$, ${}^{8,10,11}\text{B}$, ${}^{10-14}\text{C}$, ${}^{13-17}\text{N}$, ${}^{15-17,19}\text{O}$, ${}^{17}\text{F}$. Особое внимание уделяется случаям, когда основное состояние ядра не имеет гало-структуры, а возбужденное состояние может ее иметь.

Работа выполнена в Лаборатории ядерных реакций им. Г. Н. Флерова ОИЯИ.

Препринт Объединенного института ядерных исследований. Дубна, 2015

Izosimov I. N.

E6-2015-41

Isospin Quantum Number and Structure of the Excited States
in Halo Nuclei. Halo-Isomers

It has been shown that isobar-analog (IAS), double isobar-analog (DIAS), configuration (CS), and double configuration states (DCS) can simultaneously have $n-n$, $n-p$, and $p-p$ halo components in their wave functions. Differences in halo structure of the excited and ground states can result in the formation of isomers (halo-isomers). Both the Borromean and tango halo types can be observed for $n-p$ configurations of atomic nuclei. The structure of the ground and excited states with different isospin quantum number in halo-like nuclei is discussed. $B(M\lambda)$ and $B(E\lambda)$ for γ -transitions in ${}^{6-8}\text{Li}$, ${}^{8-10}\text{Be}$, ${}^{8,10,11}\text{B}$, ${}^{10-14}\text{C}$, ${}^{13-17}\text{N}$, ${}^{15-17,19}\text{O}$, and ${}^{17}\text{F}$ are analyzed. Special attention is given to nuclei whose ground state does not exhibit halo structure, but the excited state may have one.

The investigation has been performed at the Flerov Laboratory of Nuclear Reactions, JINR.

Preprint of the Joint Institute for Nuclear Research. Dubna, 2015

INTRODUCTION

Generally, the term “halo” is used when halo nucleon(s) spend(s) at least 50% of the time outside the range of the core potential, i.e., in the classically forbidden region [1–3]. The necessary conditions for the halo formation are: small binding energy of the valence particle(s), small relative angular momentum $L = 0, 1$ for two-body or hypermomentum $K = 0, 1$ for three-body halo systems, and not so high level density (small mixing with non-halo states). Coulomb barrier may suppress proton-halo formation for $Z > 10$. Neutron and proton halos have been observed in several nuclei [1–3]. In Borromean systems the two-body correlations are too weak to bind any pair of particles, while the three-body correlations are responsible for the system binding as a whole. In states with one and only one bound subsystem the bound particles moved in phase and were therefore named “tango states” [2]. Halo of Borromean type is well known in atomic nuclei [4]. The Isobar Analog State (IAS) of the ${}^6\text{He}$ ground state (two-neutron halo nucleus), i.e., the 3.56 MeV, $J = 0^+$ state of ${}^6\text{Li}$, has [5, 6] a neutron–proton halo structure of Borromean type. In the general case [7] the IAS is the coherent superposition of the excitations like neutron hole–proton particle coupled to form the momentum $J = 0^+$. The IAS has the isospin $T = T_Z + 1 = (N - Z)/2 + 1$, where $T_Z = (N - Z)/2$ is the isospin projection. The isospin of the ground state is $T = T_Z = (N - Z)/2$. When the IAS energy corresponds to the continuum, the IAS can be observed as a resonance. Configuration states (CS) are not the coherent superposition of such excitations and have $T = T_Z = (N - Z)/2$. One of the best studied CS is the antianalog state (AIAS) [7, 8]. The CS formation may be restricted by the Pauli principle. The Double Isobar Analog State (DIAS) has the isospin $T = T_Z + 2$ and is formed as the coherent superposition of the excitations like two neutron holes–two proton particles coupled to form the momentum $J = 0^+$. For the IAS, CS, DIAS, and DCS the proton particles have the same spin and spatial characteristics as the corresponding neutron holes. When the parent state is a two-neutron halo nucleus, IASs and CSs will have the proton–neutron halo structure, DIASs and the DCSs will have the proton–proton halo structure. For nuclei with enough neutron excess, IASs and CSs can have

not only the p - n halo component but also the n - n halo component, DIASs and DCSs can have both p - p , n - n and p - n components [8]. IASs, CSs, DIASs, and DCSs can be observed as resonances in nuclear reactions.

Excited halo states and resonances of non-IAS structure may also occur in atomic nuclei [2, 3, 9, 10] both from proton-rich and neutron-rich sides.

Halo of tango type is well known in molecules [2].

Characteristics of the γ -transitions in ${}^6\text{Li}$ are analyzed. It is shown that the ground state of atomic nucleus ${}^6\text{Li}$ ($J = 1^+$, $S_n = 5.66$ MeV, $S_p = 4.59$ MeV, $S_d = 1.47$ MeV) may be a good candidate for halo state of tango type.

Strong mixing with other more complicated states dilutes the component of the halo. High level density of non-halo levels prevents halo formation [2] in the excited states. In other words, the distance between non-halo states must be larger than the coupling to the halo state (or non-halo level density is not high). There may be only a small window open for halo occurrence. How small this window is can be answered by studying halo in excited states.

Isospin symmetry essentially reduced mixing of the configurations with different isospin quantum number and favorable for halo formation. Such excited states and resonances as IAS, DIAS, CS, and DCS in nuclei may simultaneously have n - n , n - p , and p - p halo components in their wave functions [8]. Differences in halo structure of the excited and ground states can result in the formation of isomers (halo-isomers). From this point of view, some CSs and DCSs, depending on their halo structure, may be observed as halo-isomers.

Structure of the ground and excited states in halo-like nuclei is discussed. Values of reduced probability $B(M\lambda)$ and $B(E\lambda)$ for γ -transitions in 6 - ${}^8\text{Li}$, 8 - ${}^{10}\text{Be}$, 8 , 10 , ${}^{11}\text{B}$, 10 - ${}^{14}\text{C}$, 13 - ${}^{17}\text{N}$, 15 - 17 , ${}^{19}\text{O}$, and ${}^{17}\text{F}$ are analyzed. Special attention is given to nuclei whose ground state does not exhibit halo structure, but the excited state may have one.

1. ISOBAR ANALOG, DOUBLE ISOBAR ANALOG, CONFIGURATION, AND DOUBLE CONFIGURATION STATES

Analog states in nuclei are of interest for both theoretical and experimental investigations. There are two main points that are decisive for the isospin T being a good quantum number in both light and heavy nuclei:

- 1) charge independence of nuclear forces acting between nucleons;
- 2) a number of factors that weaken violation of the charge independence of forces in a nucleus by Coulomb forces [7].

As a result, in a nucleus there can be (Fig. 1) several systems of levels (resonances) that differ in isospin $T(T_0, T_0 + 1, \dots)$, $T_0 = (N - Z)/2$. If $T = T_Z + 1$, these are so-called analog states; if $T = T_Z + 2$, these are double

analog states, and so on. Analog states that fall within the continuum region are also referred to as analog resonances.

Analog states for $N > Z$ ($T_Z > 0$) nuclei are formed from the initial state ($T, T = T_Z$) through various replacements of a neutron by a proton in the same state. The wave function of the analog involves excitations like proton particle–neutron hole coupled to form the momentum $J = 0^+$ which are not forbidden by the Pauli principle. Levels with the identical T are in the neighboring nuclei and are shifted relative to each other by $\Delta E_c - \delta$, where ΔE_c is the Coulomb energy of the added proton and δ is the mass difference of the neutron and the proton.

The analog structure for $N > Z$ nuclei can be obtained by applying the operator:

$$T_- = \sum a_i^+(p) a_i^-(n), \quad (1)$$

and the double analog structure is obtained by twice applying the nucleus isospin ladder operator T_- to the ground state of the parent nucleus. T_- is the operator for transformation of the neutron to the proton without a change in the function of the state in which the particle is; i.e., in (1) $a_i^-(n)$ is the operator for annihilation of the neutron in the state i , and $a_i^+(p)$ is the operator for production of the proton in the state i . By virtue of the Pauli principle, the summation is limited to the states which are filled with the neutron excess.

The wave function of the analog state is written as:

$$\psi_{T_0+1, T_0}^{\text{IAS}} = \frac{1}{\sqrt{2(T+1)}} T_- \psi_{T_0+1, T_0+1}^{\text{PS}}. \quad (2)$$

Here $\psi_{T_0+1, T_0+1}^{\text{PS}}$ is the wave function for the parent states with the isospin $T = T_0 + 1$ and the isospin projection $T_Z = T_0 + 1$ (Fig. 1). The analog state turns out to be sharply distinguished in many properties because its isospin is greater by one than the isospin of the neighboring states. The experimental and theoretical data indicate that the mixing of states with different isospins is insignificant and the individual character of analog states distinctly manifests itself in many experiments.

For nuclear ground states the isospin is equal to the isospin projection $T = T_Z = (N - Z)/2$. The analog state differs in isospin by one from the neighboring states, and the isospin of the analog state is greater by one than the isospin projection $T = T_Z + 1$. For the double analog state $T = T_Z + 2$.

The analog state is a collective state, which is a coherent superposition of elementary excitations like proton particle–neutron hole coupled to form the momentum $J = 0^+$, i.e., all elementary excitations enter into the wave function of the analog with one sign (Fig. 2). Accordingly, the double analog state is a coherent superposition of elementary excitations like two protons–two neutron holes coupled to form the momentum $J = 0^+$.

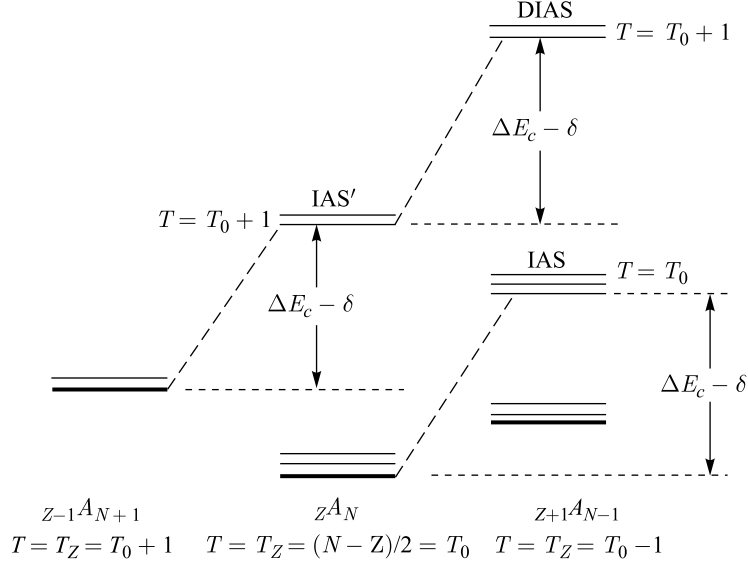


Fig. 1. Diagram of analog (IAS) and double analog (DIAS) states

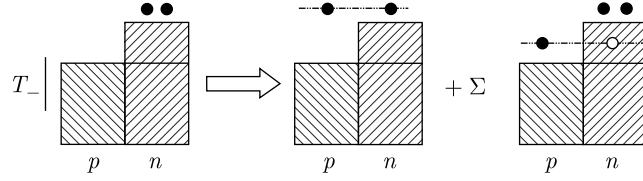


Fig. 2. Structure of the IAS wave function when the parent state has the $n-n$ halo. The IAS wave function involves two components corresponding to the $p-n$ and $n-n$ halo

If the elementary excitations enter into the wave function incoherently, the so-called configuration states are formed. In halo-like nuclei formation of configuration states can be associated with core excitation, and in some case it can be forbidden by the Pauli principle. The isospin of the configuration states is smaller than the analog isospin by one, and the excitation energy of the configuration states is also lower than the analog excitation energy. One of the best studied configuration states is (Fig. 3) the antianalog [7, 11] state (AIAS).

Since transformation of the neutron to the proton during the formation of analog, double analog, configuration, and double configuration states is not followed by a change in the spatial and spin characteristics, the above excited states in the halo-like nuclei will also have a halo-like structure.

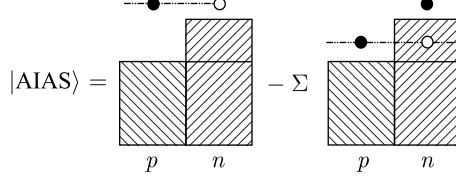


Fig. 3. Structure of the AIAS wave function when the parent state has the n halo. The antianalog wave function involves two components corresponding to the p and n halo

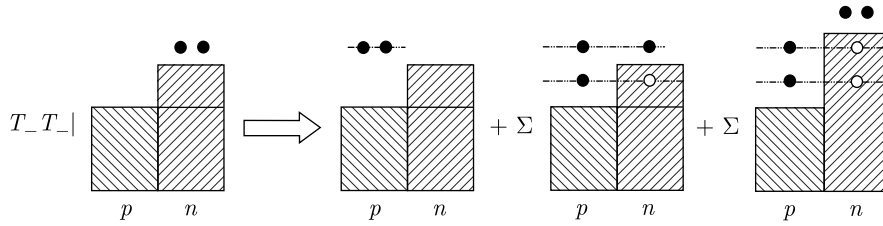


Fig. 4. Structure of the DIAS wave function when the parent state has the $n-n$ halo. The double analog wave function involves three components corresponding to the $p-p$, $p-n$, and $n-n$ halo

Let us take as the parent state the wave function for the ground state of the nucleus in which two neutrons make up the nuclear halo ($n-n$ halo) and act on it by the operator T_- (Fig. 2). As a result, we find that the wave function for the analog state and configuration states involves components corresponding to the proton-neutron halo ($n-p$ halo) and two-neutron halo ($n-n$ halo). For some nuclei configuration states are not formed by virtue of the Pauli principle, and the analog wave function can lack the component corresponding to the $n-n$ halo.

Let us act by the operator T_- on the ground state wave function for the $n-n$ halo nucleus once more (Fig. 4).

We find that the wave function for the double analog and double configuration states has the components corresponding to the $p-p$, $p-n$, and $n-n$ halo. For some nuclei there can be no $p-n$ and $n-n$ halo components by virtue of the Pauli principle. When $T_Z < 0$, all the previous reasonings and conclusions concerning nuclei with $Z > N$ remain in force under the substitution of T_- for T_+ :

$$T_+ = \sum a_i^+(n) a_i^-(p). \quad (3)$$

The corresponding configurations for nuclei with $Z > N$ are now formed under substitution of proton with neutron, which has similar spin and spatial state characteristics. Thus, in $Z > N$ nuclei, proton-particle and neutron-hole elementary excitations coupled to form the momentum $J = 0^+$ are replaced by

elementary excitations, like neutron-particle and proton-hole coupled to form the momentum $J = 0^+$. Thus, the following conclusion can be drawn [8]:

A) Such excited states and resonances as isobar analog, double isobar analog, configuration, and double configuration states in halo nuclei can also have a halo-like structure of different types ($n-n$, $p-p$, $p-n$).

B) Isobar analog, double isobar analog, configuration, and double configuration states can simultaneously have $n-n$, $n-p$, and $p-p$ halo components in their wave functions.

C) Structure of the halo may be different for the different levels and resonances in atomic nuclei.

2. CLASSIFICATION AND SYSTEMATICS OF THE γ -TRANSITIONS USING ISOSPIN

Isovector (IV) and isoscalar (IS) parts [7] may be separated in the γ -transition operator. For IV/IS γ -transition only IV/IS part of γ -transition operator gives contribution to the probability of γ -decay. Selection rules on isospin for γ -transitions are: $\Delta T = 0, \pm 1$; $\Delta T_Z = 0$. For $\Delta T = \pm 1$ only isovector part of operator gives contribution to the matrix element (IV-transitions). For $\Delta T = 0$ ($T \neq 0$) both

Table 1. Recommended [12–15] upper limits for the $B(E, \lambda)$ and $B(M, \lambda)$ in W.u.
 $\Gamma_\gamma/\Gamma_w = B(E, \lambda)/B(E, \lambda)_w$ or $B(M, \lambda)/B(M, \lambda)_w$, Γ_γ – γ -width

Transition	Γ_γ/Γ_w upper limit		
	$A = 6 - 44^a$	$A = 45 - 150$	$A > 150$
$E1$ (IV)	0.3^b	0.01	0.01
$E2$ (IS) ^c	100	300	1000
$E3$	100	100	100
$E4$	100	100^d	—
$M1$ (IV)	10	3	2
$M2$ (IV)	3	1	1
$M3$ (IV)	10	10	10
$M4$	—	30	10

Note. w — Weisskopf estimates, W.u. — Weisskopf unit.
^a Γ_γ/Γ_w (upper limit) = 10 — for $E2$ (IV); 0.03 — for $M1$ (IS); 0.1 — for $M2$ (IS); 0.003 — for $E1$ ($T = 0$ states, due to isospin mixture).
^b Γ_γ/Γ_w (upper limit) = 0.1 for $A = 21-44$.
^c In superdeformed bands $\Gamma_\gamma/\Gamma_w > 1000$ for $E2$ transitions may be observed.
^d Γ_γ/Γ_w (upper limit) = 30 for $A = 90-150$.

isovector and isoscalar parts of operator give contribution (mixture of IV and IS). For $N = Z$ ($T_Z = 0$) isovector component does not give contribution to the transitions between $T = 0$ states (IS-transitions). For $E1$ γ -decay only isovector part gives contribution to the matrix element and $E1$ γ -transitions between $T = 0$ states are forbidden on isospin in $N = Z$ nuclei. Recommended [12–15] upper limits for $B(E, \lambda)$ and $B(M, \lambda)$ are presented in Table 1. Systematics of IV/IS γ -transitions are given in [7].

In the $20 \leq A \leq 40$ nuclei contribution of the isoscalar part for γ -transitions is about: for $M1$ γ -transitions — 0.01; for $M2$ γ -transitions — 0.01; for ML , $L > 2$ γ -transitions — 0.2; for $E1$ γ -transitions — about 0.03 (T -forbidden transitions, isospin mixture about 3%).

For EL γ -transitions with $L \geq 2$ it is difficult to make some conclusion about contribution of the isoscalar part.

On isospin quantum number the γ -transitions may be classified [7] as (Table 2) favorable ($\Delta T = 1$; $T_Z = 0$), usual ($\Delta T = 0, \pm 1$; $T_Z \neq 0$), hindered ($\Delta T = 0$; $T_Z = 0$).

Table 2. Systematics of the γ -transitions in the $5 \leq A \leq 40$ nuclei [7]

<i>E1</i> γ -transitions:
A) T -allowed ($\Delta T = 1, T_Z = 0$; $\Delta T = 0, \pm 1, T_Z \neq 0$). $\langle B(E1) \rangle \approx 0.0026$ W.u.
B) T -forbidden ($\Delta T = 0, T_Z = 0$), $\langle B(E1) \rangle \approx 0.0003$ W.u., hindrance factor ≈ 7 for $N = Z$.
<i>M1</i> γ -transitions:
A) T -favorable (only IV part of γ -transition operator gives contribution, $\Delta T = \pm 1$). $\langle B(M1) \rangle \approx 0.38$ W.u.
B) T -usual (both IV and IS parts of γ -transition operator give contribution, $\Delta T = 0, T_Z \neq 0$). $\langle B(M1) \rangle \approx 0.10$ W.u.
C) T -hindered (only IS part of γ -transition operator gives contribution, $\Delta T = 0$; $T_Z = 0$). $\langle B(M1) \rangle \approx 0.0048$ W.u.
<i>M2</i> γ -transitions:
A) T -favorable. $\langle B(M2) \rangle \approx 0.31$ W.u.
B) T -hindered. $\langle B(M2) \rangle \approx 0.1$ W.u.

3. ${}^6\text{He}$ NUCLEUS (BORROMEAN n - n HALO) AND ${}^6\text{Li}$ NUCLEUS (BORROMEAN n - p HALO FOR IAS, TANGO n - p HALO FOR G.S.)

Two neutrons that form the n - n halo in ${}^6\text{He}$ ground state occupy the $1p$ orbit ($p_{3/2}$ configuration with a 7% admixture of $p_{1/2}$ configuration). The remaining two neutrons and two protons occupy the $1s$ orbit. Therefore, the action of the operator T_- on the ground state wave function for the ${}^6\text{He}$ nucleus ($T = 1$,

$T_Z = 1$) results in the formation of the analog state with the configuration corresponding to the p - n halo. This IAS is in the ${}^6\text{Li}$ nucleus ($T = 1, T_Z = 0$) at the excitation energy 3.56 MeV. The width of this state is $\Gamma = 8.2$ eV, which corresponds to the half-life $T_{1/2} = 6 \cdot 10^{-17}$ s. The experimental data [5, 6] indicate that this state has a n - p halo. Formation of configuration states is prohibited by the Pauli principle.

The γ -decay of IAS would be hindered if the ground state of ${}^6\text{Li}$ did not have a halo structure. The data on lifetime of IAS in ${}^6\text{Li}$ are given in [18], but the $M1$ γ -decay branch is not determined. If one assumes that the total lifetime of IAS is determined by $M1$ γ -decay, the reduced transition probability would be $B(M1) = 8.6$ W.u. Assuming the orbital part of the $M1$ γ -transition operator is neglected [7], $B(M1, \sigma)$ for $M1$ γ -decay of IAS in ${}^6\text{Li}$ can be determined from the reduced probability ft of the ${}^6\text{He}$ β -decay (Fig. 5). The $B(M1, \sigma)$ value proved to be 8.2 W.u., i.e., the probability of the $M1$ γ -transition is close to the value for the upper limit (Table 1) in the light nuclei region. Considerable overlap of wave functions of the two halo states (i.e., the IAS halo state and ground state halo) in ${}^6\text{Li}$ results in significant increase of the probability of $M1$ γ -transition between the states. In the absence of halo structure in the ground state of ${}^6\text{Li}$, a corresponding $M1$ γ -transition would be hindered. A rather large value of the reduced probability of $M1$ γ -transition ($B(M1, \sigma) = 8.2$ W.u.) for $M1$ γ -decay from IAS to the ground state is the evidence for the existence of tango halo structure in the ${}^6\text{Li}$ ground state. The IAS in ${}^6\text{Li}$ has the Borromean

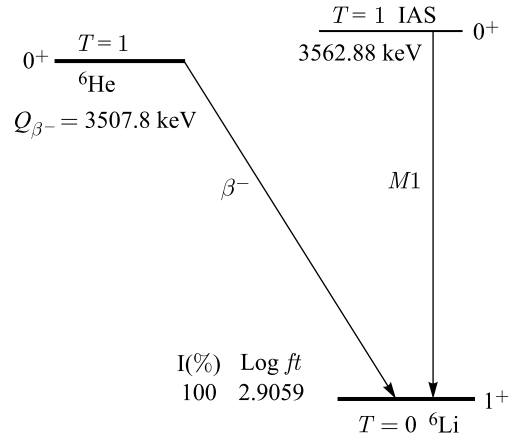


Fig. 5. Connection [7] between the ft value for β -decay of the parent state (${}^6\text{He}$ g.s.) and the $B(M1, \sigma)$ value for γ -decay of the IAS (${}^6\text{Li}$, $E = 3562$ keV). $ft = 11633/[T_0 \times B(M1, \sigma)]$, T_0 -isospin of the parent state, ft in sec, $B(M1, \sigma)$ in μ^2 , for $M1$ γ -transition W.u. = $1.79\mu^2$, $B(M1, \sigma) = 8.2$ W.u., $B(M1) \approx 8.6$ W.u.

structure since the $n-p$ subsystem is coupled to the momentum $J = 0^+$, i.e., unbound, whereas $n-p$ subsystem for the ${}^6\text{Li}$ ground state is coupled to the momentum $J = 1^+$, i.e., bound. According to halo classification [2], such structure of the ${}^6\text{Li}$ ground state corresponds to the tango halo. Such conclusion agrees with the data on the properties of ${}^6\text{Li}$ nucleus and on the properties of nuclear reactions with ${}^6\text{Li}$ beams. The radius of the ${}^6\text{Li}$ nucleus ranges between 2.32 fm and 2.45 fm, and this is 10% larger than the radius value expected from the available systematics. The ${}^6\text{Li}$ nucleus is known to have the $(\alpha + d)$ cluster structure (the energy threshold for the breakup of this nucleus into a deuteron and an alpha particle is as low as 1.47 MeV) [16, 17]. The momentum distributions of ${}^4\text{He}$ from the ${}^6\text{He}$ and ${}^6\text{Li}$ breakup were measured for different targets and beam energies. The observed momentum distributions are narrow for the ${}^6\text{He}$ breakup ($\sigma = 28-29$ MeV/ c) and intermediate for the ${}^6\text{Li}$ breakup ($\sigma = 46-55$ MeV/ c) [19, 20]. For ordinary (non-halo) nuclei, this value would have been about $\sigma = 100$ MeV/ c . The small width of the momentum distribution confirms the presence of halo in ${}^6\text{He}$, and intermediate width of the momentum distribution supports hypothesis of $n-p$ halo in ${}^6\text{Li}$ [16, 17].

4. SYSTEMATICS of the $B(M, \lambda)$ AND $B(E, \lambda)$ VALUES FOR γ -TRANSITIONS IN ${}^6-8\text{Li}$, ${}^8-10\text{Be}$, ${}^{8,10,11}\text{B}$, ${}^{10-14}\text{C}$, ${}^{13-17}\text{N}$, ${}^{15-17,19}\text{O}$, AND ${}^{17}\text{F}$. HALO ISOMERS

Data on $B(M, \lambda)$ and $B(E, \lambda)$ from [18–26] were used for the analysis of γ -transitions. The distributions of the $\lg(B(M, \lambda))$ and $\lg(B(E, \lambda))$ values for γ -transitions in ${}^6-8\text{Li}$, ${}^8-10\text{Be}$, ${}^{8,10,11}\text{B}$, ${}^{10-14}\text{C}$, ${}^{13-17}\text{N}$, ${}^{15-17,19}\text{O}$, and ${}^{17}\text{F}$ nuclei are presented in Figs. 6–15.

Systematics of the mean values $\langle B(M, \lambda) \rangle$ and $\langle B(E, \lambda) \rangle$ for these nuclei is presented in Table 3. The mean values are in agreement with previous systematics [7, 27], but one can indicate the tails for in lower $\langle \lg B(M, \lambda) \rangle$ and $\langle \lg B(E, \lambda) \rangle$ value parts of distributions. These tails may be connected with halo-isomers and they were the objects of our analysis.

When the halo structure of the excited state differs from that of the ground state, or the ground state has no halo structure, the γ -transition from the excited state to the ground state can be essentially hindered, i.e., the formation of a specific type of isomers (halo-isomers) becomes possible. The particularity of halo-isomer observations lies in the fact that it is necessary to analyze partial γ -decay lifetime.

The radial factor r^λ for the electric and $r^{\lambda-1}$ for the magnetic multipole γ -transition operator of order λ may compensate the differences in the large-distance parts of halo and no halo wave functions. Here r is the core–halo distance.

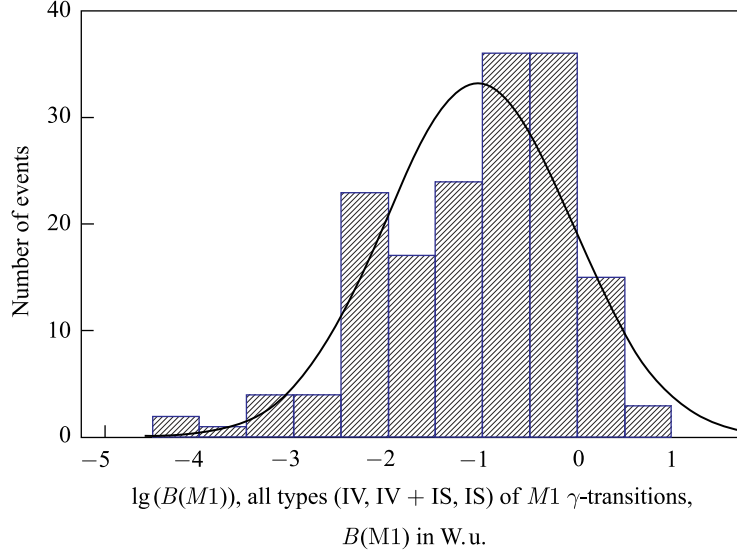


Fig. 6. Distribution of the $\lg(B(M1))$ values for IV, IV + IS, and IS $M1$ γ -transitions in ${}^6\text{-}8\text{Li}$, ${}^8\text{-}10\text{Be}$, ${}^8,10,11\text{B}$, ${}^{10-14}\text{C}$, ${}^{13-17}\text{N}$, ${}^{15-17,19}\text{O}$, and ${}^{17}\text{F}$. Mean values: $\langle \lg(B(M1)) \rangle = -1.0$, $\langle B(M1) \rangle = 0.1$ W.u., standard deviation $\sigma(\lg(B(M1))) = 0.99$

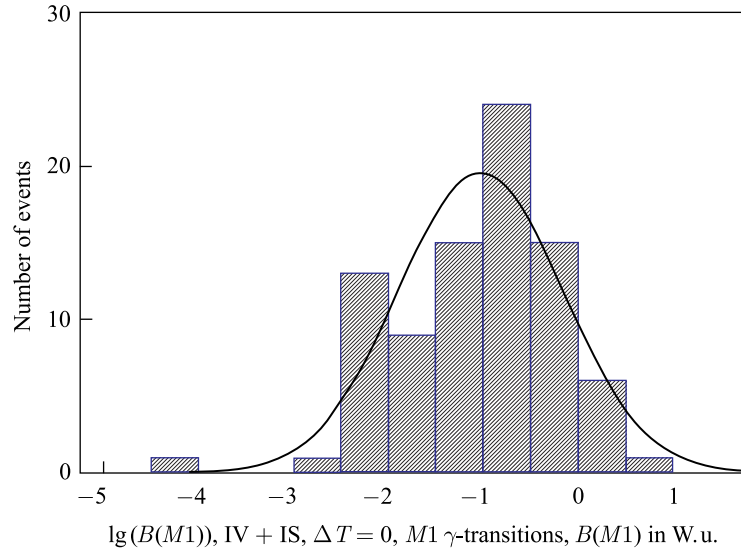


Fig. 7. Distribution of the $\lg(B(M1))$ values for $\Delta T = 0$, mixed isovector and isoscalar (IV + IS) $M1$ γ -transitions in ${}^6\text{-}8\text{Li}$, ${}^8\text{-}10\text{Be}$, ${}^8,10,11\text{B}$, ${}^{10-14}\text{C}$, ${}^{13-17}\text{N}$, ${}^{15-17,19}\text{O}$, and ${}^{17}\text{F}$. $\langle \lg(B(M1)) \rangle = -1.0$; $\langle B(M1) \rangle = 0.1$ W.u.; $\sigma(\lg(B(M1))) = 0.87$

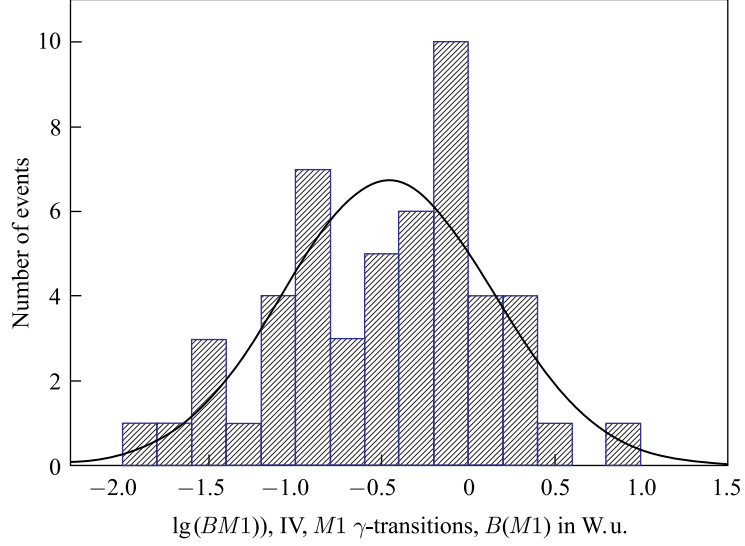


Fig. 8. Distribution of the $\lg(B(M1))$ values for $\Delta T = 1$, isovector (IV) $M1$ γ -transitions in ${}^6\text{-}8\text{Li}$, ${}^8\text{-}10\text{Be}$, ${}^8,10,11\text{B}$, ${}^{10-14}\text{C}$, ${}^{13-17}\text{N}$, ${}^{15-17,19}\text{O}$, and ${}^{17}\text{F}$. $\langle \lg(B(M1)) \rangle = -0.46$; $\langle B(M1) \rangle = 0.35$ W.u.; $\sigma(\lg(B(M1))) = 0.60$

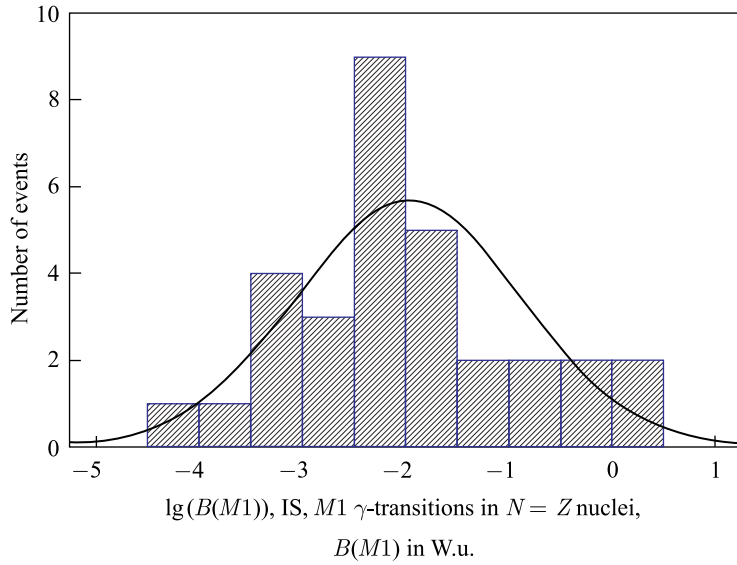


Fig. 9. Distribution of the $\lg(B(M1))$ values for isoscalar (IS) $M1$ γ -transitions in $N = Z$ nuclei ${}^6\text{Li}$, ${}^8\text{Be}$, ${}^{10}\text{B}$, ${}^{12}\text{C}$, ${}^{14}\text{N}$, and ${}^{16}\text{O}$. $\langle \lg(B(M1)) \rangle = -2.07$; $\langle B(M1) \rangle = 0.008$ W.u.; $\sigma(\lg(B(M1))) = 1.02$

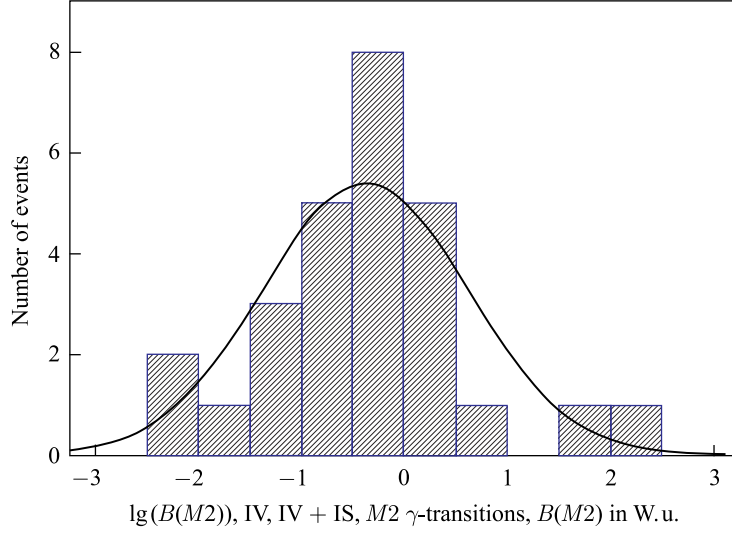


Fig. 10. Distribution of the $\lg(B(M2))$ values for IV, IV + IS, and IS M2 γ -transitions in ${}^6\text{-}^8\text{Li}$, ${}^8\text{-}^{10}\text{Be}$, ${}^8,10,11\text{B}$, ${}^{10-14}\text{C}$, ${}^{13-17}\text{N}$, ${}^{15-17,19}\text{O}$, and ${}^{17}\text{F}$. $\langle \lg(B(M2)) \rangle = -0.38$; $\langle B(M2) \rangle = 0.4$ W.u.; $\sigma(\lg(B(M2))) = 1.0$

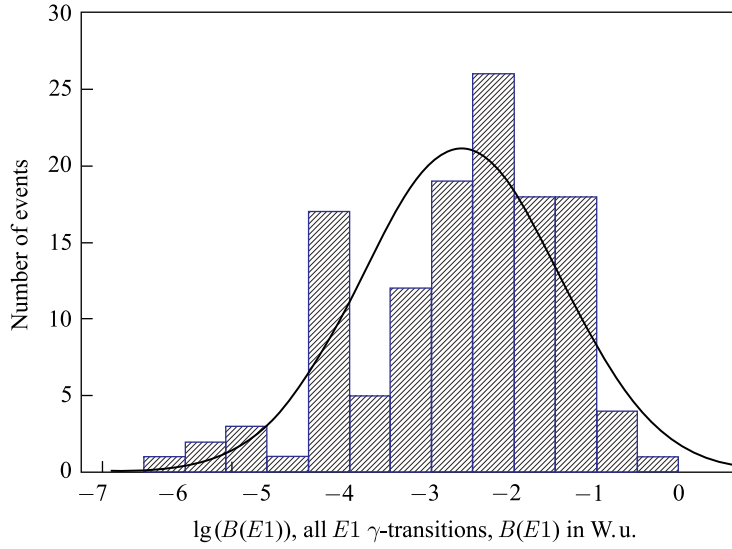


Fig. 11. Distribution of the $\lg(B(E1))$ values for all $E1$ γ -transitions in ${}^6\text{-}^8\text{Li}$, ${}^8\text{-}^{10}\text{Be}$, ${}^8,10,11\text{B}$, ${}^{10-14}\text{C}$, ${}^{13-17}\text{N}$, ${}^{15-17,19}\text{O}$, and ${}^{17}\text{F}$. $\langle \lg(B(E1)) \rangle = -2.64$; $\langle B(E1) \rangle = 0.002$ W.u.; $\sigma(\lg(B(E1))) = 1.2$

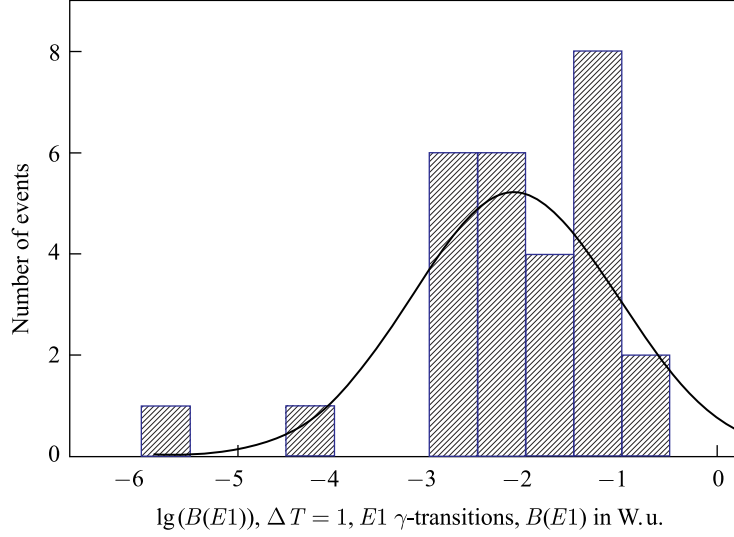


Fig. 12. Distribution of the $\lg(B(E1))$ values for $\Delta T = 1$, $E1$ γ -transitions in ${}^6\text{-}^8\text{Li}$, ${}^8\text{-}^{10}\text{Be}$, ${}^8,10,11\text{B}$, ${}^{10}\text{-}^{14}\text{C}$, ${}^{13}\text{-}^{17}\text{N}$, ${}^{15}\text{-}^{17,19}\text{O}$, and ${}^{17}\text{F}$. $\langle \lg(B(E1)) \rangle = -2.11$; $\langle B(E1) \rangle = 0.008$ W.u.; $\sigma(\lg(B(E1))) = 1.1$

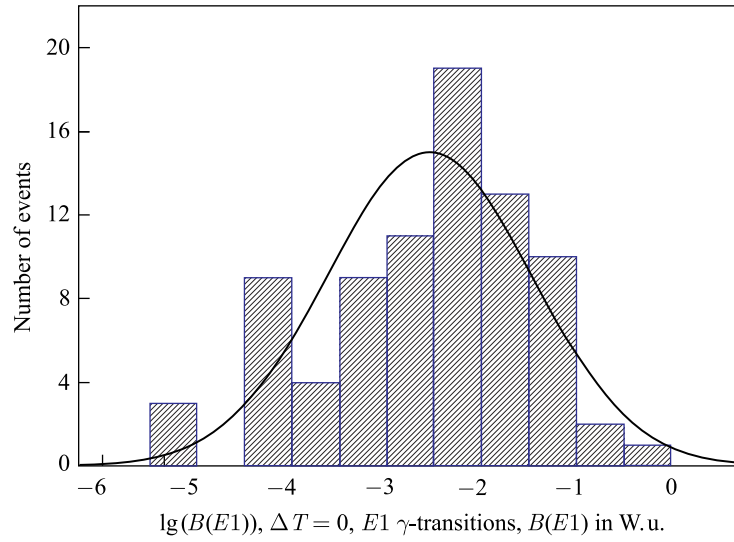


Fig. 13. Distribution of the $\lg(B(E1))$ values for $\Delta T = 0$, $E1$ γ -transitions in ${}^6\text{-}^8\text{Li}$, ${}^8\text{-}^{10}\text{Be}$, ${}^8,10,11\text{B}$, ${}^{10}\text{-}^{14}\text{C}$, ${}^{13}\text{-}^{17}\text{N}$, ${}^{15}\text{-}^{17,19}\text{O}$, and ${}^{17}\text{F}$. $\langle \lg(B(E1)) \rangle = -2.54$; $\langle B(E1) \rangle = 0.003$ W.u.; $\sigma(\lg(B(E1))) = 1.1$

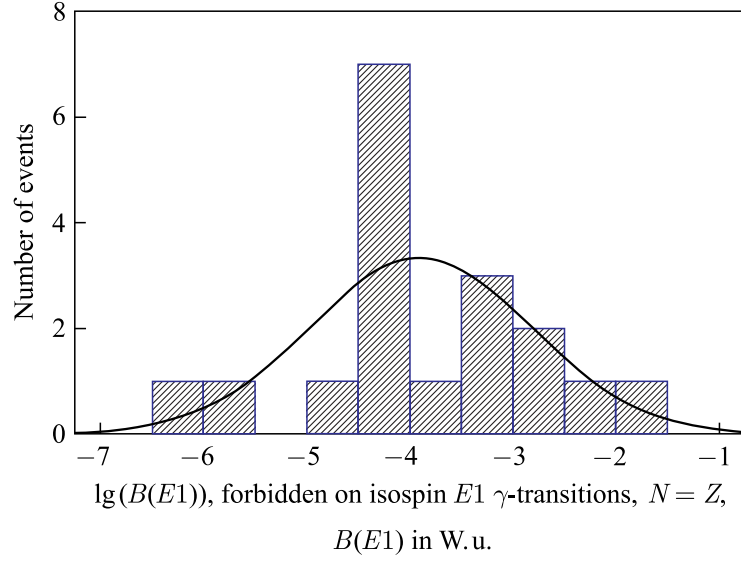


Fig. 14. Distribution of the $\lg(B(E1))$ values for forbidden on isospin $E1$ ($T = 0 \rightarrow T = 0$) γ -transitions in $N = Z$ nuclei ${}^6\text{Li}$, ${}^8\text{Be}$, ${}^{10}\text{B}$, ${}^{12}\text{C}$, ${}^{14}\text{N}$, and ${}^{16}\text{O}$. $\langle \lg(B(E1)) \rangle = -3.54$; $\langle B(E1) \rangle = 0.00029$ W.u.; $\sigma(\lg(B(E1))) = 1.32$

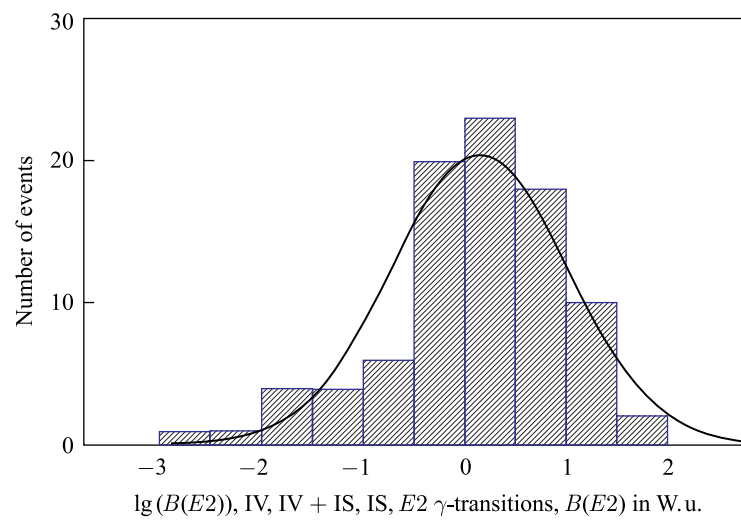


Fig. 15. Distribution of the $\lg(B(E2))$ values for IV, IV + IS, and IS $E2$ γ -transitions in ${}^6\text{--}{}^8\text{Li}$, ${}^8\text{--}{}^{10}\text{Be}$, ${}^{8,10,11}\text{B}$, ${}^{10\text{--}14}\text{C}$, ${}^{13\text{--}17}\text{N}$, ${}^{15\text{--}17,19}\text{O}$, and ${}^{17}\text{F}$. $\langle \lg(B(E2)) \rangle = 0.15$; $\langle B(E2) \rangle = 1.4$ W.u.; $\sigma(\lg(B(E2))) = 0.87$

Table 3. Systematics of the mean values $\langle B(M, \lambda) \rangle$ and $\langle B(E, \lambda) \rangle$ for γ -transitions in ${}^6\text{-}8\text{Li}$, ${}^8\text{-}10\text{Be}$, ${}^8,10,11\text{B}$, ${}^{10-14}\text{C}$, ${}^{13-17}\text{N}$, ${}^{15-17,19}\text{O}$, and ${}^{17}\text{F}$ nuclei. IS/IV — isoscalar/isovector transitions

<p><i>E1</i>-transitions:</p> <p>A) <i>T</i>-favorable, $\Delta T = \pm 1$. $\langle B(E1) \rangle \approx 0.0079$ W.u. B) <i>T</i>-usual, $\Delta T = 0$; $T_Z \neq 0$. $\langle B(E1) \rangle \approx 0.0032$ W.u. C) <i>T</i>-forbidden, $\Delta T = 0$; $T_Z = 0$. $\langle B(E1) \rangle \approx 0.00029$ W.u. <i>T</i>-allowed, $\Delta T = 1$; $T_Z = 0$. $\langle B(E1) \rangle \approx 0.006$ W.u. <i>T</i>-forbidden factor ≈ 20 D) All, $\Delta T = 0, \pm 1$; $\Delta T_Z = 0$. $\langle B(E1) \rangle \approx 0.0025$ W.u.</p>
<p><i>E2</i>-transitions:</p> <p>A) $\Delta T = \pm 1$, $T_Z \neq 0$. $\langle B(E2) \rangle \approx 1.51$ W.u. B) $\Delta T = 0$; $T_Z \neq 0$. $\langle B(E2) \rangle \approx 1.29$ W.u. C) $\Delta T = 0$; $T_Z = 0$. $\langle B(E2) \rangle \approx 1.3$ W.u. D) $\Delta T = \pm 1$; $\Delta T_Z = 0$. $\langle B(E2) \rangle \approx 1.2$ W.u.</p>
<p><i>E3</i>-transitions:</p> <p>A) $\Delta T = 0$; $T_Z \neq 0$. $\langle B(E3) \rangle \approx 4$ W.u. B) $\Delta T = 0$; $T_Z = 0$. $\langle B(E3) \rangle \approx 8$ W.u. C) $\Delta T = 0$; $\Delta T_Z = 0$. $\langle B(E3) \rangle \approx 5$ W.u.</p>
<p><i>M1</i>-transitions:</p> <p>A) <i>T</i>-favorable, $\Delta T = \pm 1$. $\langle B(M1) \rangle \approx 0.35$ W.u. B) <i>T</i>-usual, $\Delta T = 0$. $\langle B(M1) \rangle \approx 0.1$ W.u. C) <i>T</i>-hindered (IS), $\Delta T = 0$; $T_Z = 0$. $\langle B(M1) \rangle \approx 0.008$ W.u. <i>T</i>-favorable (IV), $\Delta T = 1$; $T_Z = 0$. $\langle B(M1) \rangle \approx 0.2$ W.u. Hindrance factor ≈ 20 for IS transitions D) All, $\Delta T = 0, \pm 1$; $\Delta T_Z = 0$. $\langle B(M1) \rangle \approx 0.1$ W.u.</p>
<p><i>M2</i>-transitions:</p> <p>A) <i>T</i>-favorable, $\Delta T = \pm 1$. $\langle B(M2) \rangle \approx 1.23$ W.u. B) <i>T</i>-usual, $\Delta T = 0$; $T_Z \neq 0$. $\langle B(M2) \rangle \approx 0.42$ W.u. C) <i>T</i>-hindered (IS), $\Delta T = 0$; $T_Z = 0$. $\langle B(M2) \rangle \approx 0.056$ W.u. <i>T</i>-favorable (IV), $\Delta T = \pm 1$; $\Delta T_Z = 0$. $\langle B(M2) \rangle \approx 1.9$ W.u. Hindrance factor ≈ 30 for IS transitions</p>

The most sensitive for detection of the γ -transition hindrance between halo–no halo states will be *M1* γ -transitions (or may be *E1* and *M2*).

It is necessary to have proper consideration of the soft mode [1–3] with different multipolarity for halo states and halo–halo γ -transitions.

Up to now the halo structure has been detected for fairly considerable number of nuclei, and the list of halo nuclei continues to expand. The following halo nuclei have been selected as an initial (parent (2)) nucleus in isobar chains:

Table 4. Halo (intermediate halo) \rightarrow halo (intermediate halo) γ -transitions.
 $[T_{1/2}(\text{s}) \times \Gamma(\text{eV})] = 4.8 \cdot 10^{-16}$

No.	Nuclei/ γ -transition
1.	${}^6\text{Li}$, IAS, $E_{\text{lev}} = 3.56$ MeV(resonance), $I^\pi = 0^+$, $T = 1 \rightarrow {}^6\text{Li}$, g.s., $I^\pi = 1^+$, $T = 0$, $S_n = 5665$ keV, $S_p = 4593$ keV, $S_d = 1474$ keV. $B(M1) = 8.6$ W.u., $T_{1/2} = 5.9 \cdot 10^{-17}$ s
2.	${}^9\text{Be}$, $S_n = 1665.4$ keV, $S_p = 16888.2$ keV; $E_{\text{lev}} = 1.68$ MeV (resonance), $I^\pi = 1/2^+ \rightarrow$ g.s., $I^\pi = 3/2^-$, $B(E1) = 0.22$ W.u., $\Gamma_\gamma = 0.30$ eV
3.	${}^8\text{B}$, $S_n = 13020$ keV, $S_p = 137.5$ keV; $E_{\text{lev}} = 0.7695$ MeV (resonance), $I^\pi = 1^+$, $\Gamma_\gamma = 0.0252$ eV \rightarrow g.s., $I^\pi = 2^+$, $B(M1) = 2.63$ W.u.
4.	${}^{10}\text{C}$, $S_n = 21283.1$ keV, $S_p = 4006.0$ keV, $S_{2p} = 3820.9$ keV; $E_{\text{lev}} = 3.3536$ MeV, $I^\pi = 2^+$, \rightarrow g.s., $I^\pi = 0^+$, $B(E2) = 9.6$ W.u. $T_{1/2} = 155$ fs ($4.25 \cdot 10^{-3}$ eV)
5.	${}^{10}\text{Be}$, $S_n = 6812$ keV, $S_p = 19636$ keV; $E_{\text{lev}} = 7371$ keV (resonance), $I^\pi = 3^- \rightarrow E_{\text{lev}} = 5958$ keV, $I^\pi = 2^+$, $B(E1) = 0.12$ W.u., $\Gamma_\gamma = 0.11$ eV
6.	${}^{11}\text{Be}$, $S_n = 501.62$ keV, $S_p = 20165$ keV; $E_{\text{lev}} = 320$ keV, $I^\pi = 1/2^- \rightarrow$ g.s., $I^\pi = 1/2^+$, $B(E1) = 0.36$ W.u., $T_{1/2} = 115$ fs
7.	${}^{10}\text{B}$, $S_n = 8436.3$ keV, $S_p = 6585.9$ keV; $E_{\text{lev}} = 6875$ KeV (resonance), $I^\pi = 1^-$, $T = 0 + 1$ (mixture) $\rightarrow E_{\text{lev}} = 5919$ keV, $I^\pi = 2^+$, $T = 0$, $B(E1) = 0.19$ W.u. (due to isospin mixture), $\Gamma_\gamma = 0.054$ eV
8.	${}^{17}\text{F}$, $S_n = 16800$ keV, $S_p = 600.27$ keV; $E_{\text{lev}} = 495$ keV, $I^\pi = 1/2^+ \rightarrow$ g.s., $I^\pi = 5/2^+$, $B(E2) = 25$ W.u. $T_{1/2} = 286$ ps

n - n halo — ${}^6\text{He}$, ${}^{11}\text{Li}$, ${}^{12,14}\text{Be}$, ${}^{17}\text{B}$; p - n halo — ${}^6\text{Li}$; n halo — ${}^{11}\text{Be}$, ${}^{14}\text{B}$, ${}^{17,19}\text{C}$; p - p halo — ${}^{10}\text{C}$, ${}^{17}\text{Ne}$; p halo — ${}^8\text{B}$, ${}^{12}\text{N}$, ${}^{17}\text{F}$. Using an available body of evidence [18–26] on γ -decay for $6 \leq A \leq 17$ nuclei, we selected halo (intermediate halo)–halo (intermediate halo) γ -transitions. $B(M, \lambda)$ and $B(E, \lambda)$ (Table 4) for such types of γ -transitions are fairly large near the upper limit (Table 2) within selected nuclear region. This implies high overlapping (especially for $M1$ transitions) of wave functions of the initial and final states of nuclei undergoing γ -transition.

As a next step, we selected excited states of nuclei whose characteristics were suitable for halo formation (low binding energy and angular momentum), γ -decay was hindered, multipolarity of transitions was small, and the final state of γ -decay had *a fortiori* a non-halo structure (large binding energy). The data on γ -decay of halo (intermediate halo)–non-halo type are presented in Table 5.

The comparison of data from Tables 4 and 5 shows that the reduced probabilities of halo–non-halo γ -transitions (Table 5) are far lower than those of halo–halo γ -transitions (Table 4). The hindrance factor can reach 10^4 for $M1$ γ -transitions, $5 \cdot 10^4$ for $E1$ γ -transitions, and 10^2 for $E2$ γ -transitions.

Table 5. Halo (intermediate halo) \rightarrow no halo γ -transitions

No.	Nuclei/ γ -transition
1.	^{10}B , $S_n = 8436.3$ keV, $S_p = 6585.9$ keV; $E_{\text{lev}} = 5919$ keV, $I^\pi = 2^+$ \rightarrow g.s., $I^\pi = 3^+$, $B(M1) = 0.026$ W.u. $\Gamma_\gamma = 0.112$ eV; $\rightarrow E_{\text{lev}} = 718$ keV, $I^\pi = 1^+$, $B(M1) = 0.0085$ W.u., $\Gamma_\gamma = 0.025$ eV.
2.	^{10}Be , $S_n = 6812$ keV, $S_p = 19636$ keV; $E_{\text{lev}} = 5958.39$ keV, $I^\pi = 2^+$, $T_{1/2} \leq 55$ fs ($> 90\%$) $\rightarrow E_{\text{lev}} = 3368$ keV, $I^\pi = 2^+$, $B(M1) \approx 0.03$ W.u.
3.	^{14}N , $S_n = 10553.3$ keV, $S_p = 7550.6$ keV; $E_{\text{lev}} = 6.20$ MeV, $I^\pi = 1^+$ \rightarrow g.s., $I^\pi = 1^+$, $B(E2) = 0.021$ W.u., $B(M1) = 0.0018$ W.u., $T_{1/2} = 160$ fs.
4.	^{14}N , $S_n = 10553.3$ keV, $S_p = 7550.6$ keV; $E_{\text{lev}} = 9.13$ MeV (resonance), $I^\pi = 3^+$, $T_{1/2}(\gamma) = 45$ fs \rightarrow g.s., $I^\pi = 1^+$, $B(E2) = 0.0081$ W.u.; $\rightarrow E_{\text{lev}} = 5.83$ MeV, $I^\pi = 3^-$, $B(E1) = 6.4 \cdot 10^{-5}$ W.u.; $\rightarrow E_{\text{lev}} = 6.45$ MeV, $I^\pi = 3^+$, $B(M1) = 2.2 \cdot 10^{-3}$ W.u.
5.	^{14}N , $S_n = 10553.3$ keV, $S_p = 7550.6$ keV; $E_{\text{lev}} = 9.70$ MeV (resonance), $I^\pi = 1^+$, $\Gamma_\gamma = 0.06$ eV \rightarrow g.s., $I^\pi = 1^+$, $B(M1) = 0.00094$ W.u.; $\rightarrow E_{\text{lev}} = 2.31$ MeV, $I^\pi = 0^+$, $T = 1$, $B(M1) = 5.1 \cdot 10^{-3}$ W.u.

CONCLUSIONS

1. Such excited states and resonances as isobar analog, double isobar analog, configuration, and double configuration states in halo nuclei can also have a halo-like structure of different types ($n-n$, $p-p$, $p-n$).

2. Isobar analog, double isobar analog, configuration, and double configuration states can simultaneously have $n-n$, $n-p$, and $p-p$ halo components in their wave functions.

3. The ground state of atomic nucleus ^6Li ($J = 1^+$, $S_n = 5.66$ MeV, $S_p = 4.59$ MeV, $S_d = 1.47$ MeV) is a good candidate for halo state of tango type. A large value of the reduced probability of $M1$ γ -transition from IAS to the ground state is the evidence for the existence of tango halo structure in the ^6Li ground state.

4. For $A = 6-19$ nuclei the hindrance factor of $M1$ γ -transitions is up to 10000 for halo \rightarrow no halo in comparison with halo \rightarrow halo γ -transitions, hindrance factor of $E1$ γ -transitions is up to 50000 for halo \rightarrow no halo in comparison with halo \rightarrow halo γ -transitions, hindrance factor of $E2$ γ -transitions is up to 100 for halo \rightarrow no halo in comparison with halo-halo γ -transitions.

6. Differences in halo structure of the excited and ground states can result in the formation of isomers (halo-isomers).

REFERENCES

1. *Tanihata I.* Neutron Halo Nuclei // *J. Phys. G: Nucl. Part. Phys.* 1996. V. 22. P. 157.
2. *Jensen A. S. et al.* Structure and Reactions of Quantum Halos // *Rev. Mod. Phys.* 2004. V. 76. P. 215.
3. *Jonson B.* Light Dripline Nuclei // *Phys. Rep.* 2004. V. 389. P. 1.
4. *Zhukov M. V. et al.* Bound State Properties of Borromean Halo Nuclei: ${}^6\text{He}$ and ${}^{11}\text{Li}$ // *Phys. Rep.* 1993. V. 231. P. 151.
5. *Suzuki Y., Yabana K.* Isobaric Analogue Halo States // *Phys. Lett. B.* 1991. V. 272. P. 173.
6. *Zhihong L. et al.* First Observation of Neutron-Proton Halo Structure for the 3.563 MeV 0^+ State in ${}^6\text{Li}$ via ${}^1\text{H}({}^6\text{He}, {}^6\text{Li})n$ Reaction // *Phys. Lett. B.* 2002. V. 527. P. 50.
7. *Naumov Yu. V., Kraft O. E.* Isospin in Nuclear Physics, Nauka, Moscow, Leningrad, 1972.
8. *Izosimov I. N.* Structure of the Isobar Analog States (IAS), Double Isobar Analog States (DIAS), and Configuration States (CS) in Halo Nuclei // *Proc. Int. Conf. EXON2012, Vladivostok, Russia, World Scientific, 2013. P. 129. Joint Institute for Nuclear Research Preprint E6-2012-121, Dubna (2012).*
9. *Ogloblin A. A. et al.* Observation of Neutron Halos in the Excited States of Nuclei // *Int. Journ. of Mod. Physics E.* 2011. V. 20. P. 823.
10. *Chen Jin-Gen. et al.* Proton Halo or Skin in the Excited States of Light Nuclei // *Chin. Phys. Lett.* 2003. V. 20. P. 1021.
11. *Naumov Yu. V., Kraft O. E.* Gamma-Decay of the Analogue Resonances // *Phys. Part. Nucl.* 1975. V. 6. P. 892.
12. *Tuli J. K.* Evaluated Nuclear Structure Data File: A Manual for Preparation of Data Sets // *Rep. BNL-NCS-51655-01/02-Rev.* 2001.
13. *Endt P. M.* Strengths of Gamma-Ray Transitions in $A = 45-90$ Nuclei // *At. Data Nucl. Data Tables.* 1979. V. 23. P. 547.
14. *Endt P. M.* Strengths of Gamma-Ray Transitions in $A = 6-44$ Nuclei (III) // *Ibid.* P. 3.
15. *Endt P. M.* Strengths of Gamma-Ray Transitions in $A = 91-150$ Nuclei // *At. Data Nucl. Data Tables.* 1981. V. 26. P. 47.
16. *Kalpakchieva R. et al.* Momentum Distributions of ${}^4\text{He}$ Nuclei from the ${}^6\text{He}$ and ${}^6\text{Li}$ Breakup // *Phys. At. Nucl.* 2007. V. 70. P. 619.
17. *Penionzhkevich Yu. E.* Special Features of Nuclear Reactions Induced by Loosely Bound ${}^6\text{He}$ and ${}^{6,7}\text{Li}$ Nuclei in the Vicinity of the Coulomb Barrier Height // *Phys. At. Nucl.* 2009. V. 72. P. 1617.
18. <http://www.nndc.bnl.gov>
19. *Tilley D. R. et al.* Energy Levels of Light Nuclei $A = 6$ // *Nucl. Phys. A.* 2002. V. 708. P. 3.
20. *Kelley J. H. et al.* Energy Levels of Light Nuclei $A = 11$ // *Nucl. Phys. A.* 2012. V. 880. P. 88.

21. *Tilley D. R. et al.* Energy Levels of Light Nuclei $A = 5, 6, 7$ // Nucl. Phys. A. 2002. V. 708. P. 3.
22. *Tilley D. R. et al.* Energy Levels of Light Nuclei $A = 8, 9, 10$ // Nucl. Phys. A. 2004. V. 745. P. 155.
23. *Ajzenberg-Selove F.* Energy Levels of Light Nuclei $A = 11-12$ // Nucl. Phys. A. 1990. V. 506. P. 1.
24. *Ajzenberg-Selove F.* Energy Levels of Light Nuclei $A = 13-15$ // Nucl. Phys. A. 1991. V. 523. P. 1.
25. *Tilley D. R. et al.* Energy Levels of Light Nuclei $A = 16-17$ // Nucl. Phys. A. 1993. V. 565. P. 1.
26. *Tilley D. R. et al.* Energy Levels of Light Nuclei $A = 18-19$ // Nucl. Phys. A. 1995. V. 595. P. 1.
27. *Soloviev V. G.* Theory of Atomic Nuclei: Quasiparticles and Phonons, Institute of Physics, Bristol and Philadelphia, 1992.

Received on May 26, 2015.

Редактор *Е. И. Крупко*

Подписано в печать 20.07.2015.

Формат 60 × 90/16. Бумага офсетная. Печать офсетная.

Усл. печ. л. 1,25. Уч.-изд. л. 1,48. Тираж 225 экз. Заказ № 58593.

Издательский отдел Объединенного института ядерных исследований
141980, г. Дубна, Московская обл., ул. Жолио-Кюри, 6.

E-mail: publish@jinr.ru

www.jinr.ru/publish/